18th International Conference on Structural Mechanics in Reactor Technology (SMiRT 18)
Beijing, China, August 7-12, 2005
SMiRT18-W01-2

SHAFT SHOCK ABSORBER FOR A SPENT FUEL CANISTER

Tapani Kukkola
Fortum Nuclear Services Ltd
POB 100, 00048 FORTUM, Finland
E-mail: tapani.kukkola@fortum.com

ABSTRACT

The disposal canister for spent nuclear fuel will be transferred by a lift to the repository which is 500m deep in the bedrock.

Model tests were carried out with an objective to estimate weather feasible shock absorber can be developed against the design accident case where the canister should survive a free fall to the lift shaft. If the velocity of the canister is not controlled by air drag or by any other deceleration means, the impact velocity may reach ultimate speed of 100m/s.

The canister would retain its integrity in impact on water when the bottom pit of the lift well is filled with groundwater. However, the canister would hit the pit bottom with high velocity since the water hardly slows down the canister. The impact to the bottom of the pit should be dampened mechanically.

The tests demonstrated that 20m high filling to the bottom pit of the lift well by Light Expanded Clay Aggregate (LECA), gives fair impact absorption to protect the fuel canister. Presence of ground water is not harmful for impact absorption system provided that the ceramic gravel is not floating too high from the pit bottom. Almost ideal impact absorption conditions are met if the water high level does not exceed two thirds of the height of the gravel.

Shaping of the bottom head of the cylindrical canister does not give meaningful advantages to the impact absorption system. The flat nose bottom head of the fuel canister gives adequate deceleration properties.

Keywords: spent nuclear fuel disposal, fuel canister, canister transport, drop shock absorber.

1. INTRODUCTION

1.1 General

The spent nuclear fuel will be disposed at the depth of half kilometer in bedrock. The fuel assemblies are enclosed before disposal in the composite canister, which has the cast iron insert and 50 mm thick copper sleeve. The weigh of the fuel canister with the fuel is about 25 tons. The fuel canisters are transferred into the repository by the lift. The disposal work starts in Eurajoki at Olkiluoto site in year 2020.

1.2 Definition of accident situation

All canister lift ropes are broken and the lift cage with the fuel canister is fallen into the lift shaft. It is assumed that elevator guide rails control the cage movement in first phase of the fall and the fuel canister is in vertical position in the fall into the shaft.

The depth of the shaft is 500 meters and there is 20 meters ground water column at the bottom of the shaft. The canister shaft diameter is 6.5 m. The lift cage with the fuel canister is impacting on the water. The fuel canister with the automated guided vehicle (canister trolley) is penetrating the lift cage floor.

The impact shall be dampened so that the fuel canister remains intact. The shock absorber is to be designed to guarantee as even as possible braking force. It can be proven that the fuel canister remains intact if the canister is decelerated along 10 meters distance in water. This subtends of 14 MPa's pressure at the bottom of the fuel canister.

An objective is to create simple, completely reliable shock absorber, which dampens the canister impact so that the canister remains intact. The shock absorber shall not hinder the disposal facility operations, the shock absorber shall be passive and the costs of the shock absorber should be marginal compared with other costs. The canister shaft bottom can be made 10 to 15 meters deeper, for example, the canister shaft bottom can be reshaped and the canister shaft bottom diameter can be reduced, if necessary.

1.3 Initial data for tests

The maximum impact velocity could be in theory 100 m/s. The lift cage speed is limited by drag. However, the fall is studied without any braking effects. Also the counterweight and the lift ropes are ignored.

The fuel canister outer diameter is 1.050 m, the length of caniste is 4.8 m and the canister full weight is 24.5 tons for the Olkiluoto plant fuel. The Loviisa plant fuel canister diameter is the same as Olkiluoto fuel canister, the canister length is 3.6 m and the disposal ready canister's weight is 18.7 tons.

The Olkiluoto third unit fuel canister is longer and its weight is larger than Olkiluoto first and second unit fuel canister. The shock absorber shall be capable to damp also the impact of the heavier canister.

The experimental tests will be made in scale 1:16. The tests were performed in Fortum's Hydro Laboratory in HELSINKI by Fortum Nuclear Services Ltd (FNS) under assignment of POSIVA Oy.

1.4 General questions

What is the terminal velocity of an object in the fall in open water? Water may not damp the fall and the terminal velocity remains too high. The terminal velocity is reached when the gravity force equals the drag force added by the buoyancy force. What is effect of the scale factor to the terminal velocity? Calculated terminal velocities may be the basis for determination of the scale factor. Also the object shape affects to the terminal velocity. Dimensionless drag coefficient C_D represents the shape dependent drag force. What is the distance the terminal velocity is reached after water entry? What are the pressures and decelerations in the impact? What are the maximum pressure and deceleration durations?

Four different phases can be identified in the canister impact process:

- Impact on water
- Water entry
- Deceleration to the terminal velocity
- Impact on the shaft bottom

1.5 Test measurements

In the tests the following things will be measured or clarified:

- Does the object withstand the impact on water?
- What is the maximum pressure at the impact phase? (If the duration of maximum pressure is very short-term then even very high pressure has only small effect).
- What is the maximum deceleration in the impact phase?
- How the object is decelerating in water entry?
- How the object motion is decelerating in water?
- Does the object reach the terminal velocity before impact on shaft bottom?
- What is the impact velocity at the shaft bottom?
- To develop the shaft bottom shock absorber and its performance measurements.

2. THEORETICAL BASES

2.1 Terminal velocity

The terminal velocity is reached when the gravity force equals the resistance forces (Munson et al. 1990), i.e. Equation 1:

$$W = Drag + F_b \qquad \text{Eq. 1}$$

Where W is the gravity force, Drag is the drag force and F_b is the buoyant force. The object is cylindrical with diameter D, height h and density ρ_c. The water density is ρ_w. The terminal velocity v can be solved by Equation 2:

$$v = \sqrt{\frac{2 * h(\rho_c - \rho_w) / \rho_w * g}{C_D}} \qquad \text{Eq. 2}$$

The terminal velocity in water is comparable on the square root of the scale factor. The drag coefficient C_D is composed of two factors; friction drag coefficient C_{Df} and pressure drag coefficient C_{Dp}. Drag coefficient C_D depends on the shape of the object and from the Reynolds number. If the Reynolds number is large then share of the friction drag is negligible; with Reynolds numbers 10^3, 10^4 and 10^5 the friction drag coefficients are 0.138, 0.0483 and 0.0158 respectively for the cylindrical object transversely in the flow, (Munson et al. p. 608 (1990).

When the relation of the object height and diameter is 4 and the Reynolds number is larger than 10^5 then the drag coefficient 0.85 for the cylindrical object transversely in the flow is received, Munson et al. p. 628 (1990). Then the terminal velocity formula gives 27.4 m/s for the fuel canister. The terminal velocity is in water too large. The speed of the canister in water shall be slowed down.

2.2 Entry into water

Entry into water is investigated in reference by Sedov (1982) and by Kornhauser (1962).

2.2.1 Shock pressure

The impact pressure p with impact speed less than 100 m/s is received by Equation 3, Kornhauser (1962):

$$p = \rho_0 C_0 v \qquad \text{Eq. 3}$$

In where ρ_0 is water volume density, C_0 is the speed of sound in water (about 1500 m/s) and v is impact velocity. The impact pressure with impact speed of 100 m/s is about 150 MPa and with the impact speed of 25 m/s about 38 MPa. The duration of the impact pressure is extremely short-term.

2.2.2 Deceleration in water entry

The maximum deceleration $\ddot{y}$ during the water entry can be calculated by Equation 4, Kornhauser (1962):

$$\ddot{y} = \frac{3}{8} C_p v_0^2 / (r\gamma) \qquad \text{Eq. 4}$$

In where C_p is impact drag coefficient, v_0 is impact velocity, r is the diameter of the object and γ is the ballistic density factor, which is calculated by Equation 5:

$$\gamma = W / (\frac{4}{3}\pi \rho_0 r^3) \qquad \text{Eq. 5}$$

In where W is the object's weight and r is the object's radius. Velocity loss during the water entry can be calculated by Equation 6, Kornhauser (1962):

$$\frac{\Delta v}{v_0} = 1 - e^{-\gamma/4} \qquad \text{Eq. 6}$$

When the object weight is 5.2 kg and the radius 0.03 m then the ballistic density factor γ is 46. This yields about 16 g maximum deceleration with the impact velocity of 25 m/s when factor C_p is assumed to be 1.0, conservatively. When the object weight is 25000 kg, radius 0.5 m and the impact velocity is 100 m/s, then maximum deceleration is the same as above. This also partially proves that the impact velocity 25 m/s in scale tests subtends the velocity 100 m/s in real scale. The velocity loss of the object in water entry is negligible.

2.3 Deceleration in water

Water resists the object entry into water. The maximum deceleration can be calculated by Equation 7, Kornhauser (1962):

$$\ddot{y} = \frac{3}{8} C_D v^2 /(r\gamma) \qquad \text{Eq. 7}$$

Which is the same equation as above except the drag coefficient C_D is different. The drag coefficient C_D value for the object with flat nose is about 0.9 when the speed is between 120-150 m/s, Kornhauser p. 35 (1962).

The vertical movement of an object is described by the formula in where all forces acting on the object are enclosed. The product of mass and acceleration equals with the gravity force reduced by drag force and buoyancy force, Equation 8:

$$ma = mg - Fb - Drag \qquad \text{Eq. 8}$$

By substituting the mass, buoyancy and drag terms into the formula and by notating that the acceleration and the velocity are second and first order displacement's derivatives, Equation 9:

$$\rho_c \frac{\pi D^2}{4} h * g * \ddot{X} = \rho_c \frac{\pi D^2}{4} h * g - \rho_w \frac{\pi D^2}{4} h * g - 1/2 * \rho_w \dot{X}^2 * \pi D^2 / 4 * C_D \qquad \text{Eq. 9}$$

The equation can be solved numerically for example with help of finite difference method by replacing the derivatives by displacement differences. The equation can be solved numerically with help of a simple computer program. The displacements, velocities and accelerations are calculated as a function of time.

Figure 1 shows the calculated velocity history as a function of time in real scale. The violet curve shows the velocity history from static state. The yellow curve shows the velocity history at 100 m/s impact speed and blue curve velocity history at 75 m/s impact speed. The curves meet at the same point. The terminal velocity is reached about in 5 seconds.

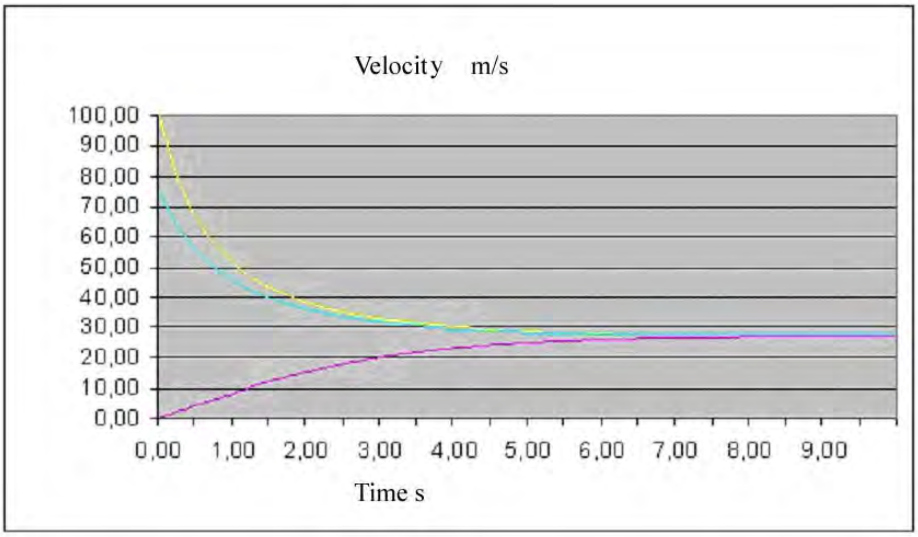

Fig.1 Velocity histories in real scale.

The deceleration at the moment of 0.05 seconds is about 100 m/s^2. In 5 seconds the displacements are about 100 to 200 meters, thus water does not damp enough the velocities.

2.4 Crash to shaft bottom

The fuel canister impact at the shaft bottom is severe unless the shaft diameter is not reduced. Canister impact on the shaft bottom shall be damped by the mechanical shock absorber in any cases. The most essential target of the tests is to create proper shock absorber on the shaft bottom. The calculated impact velocity on the shaft bottom is 80 m/s when the impact velocity on water is 100 m/s. The calculated maximum deceleration during travel through water below remains below 10 g.

2.5 Scale factor

The test velocity should be the real velocity divided by square root of scale as shown in previous considerations. When the real velocity is 100 m/s and scale is 1:16 then the test velocity should be 25 m/s.

3. TEST ARRANGEMENTS

3.1 Pre-test arrangements

Pre-tests were made in order to experiment the test arrangement and the measurement systems. Two canister models were made from steel tube with welded flat end plates. Model 1 is in scale 1:16.7, length is 300 mm and the diameter 60 mm. Model 2 is in scale 11.1, length is 450 mm and the diameter is 90 mm. The weight of both models is 5.2 kg. Photographs of the models are shown in Figure 2.

Fig. 2 Photos of the canister models; left Model 1 and right Model 2.

Figure 3 (right) shows the canister sling. The frame of the canister sling is made from square pipes. Four guide tracks are installed in the center of framework. The test piece is fixed in the sledge, which moves along the guide tracks. The sledge is accelerated by a tackle gear. The driving force for the tackle gear is given by the four rubber belt bundles, shown yellow in center of Figure 3. The tackle gear is tensioned with help of the 2.5 tons capacity bridge crane of the test hall. The maximum tensioning force of the tackle gear is about 15 kN. Figure 3 (left, upper) shows the test piece holder. The trigger logout level is shown right in Figure 3 (left, lower).

Fig. 3 Canister sling (right), test piece holder (left upper) and trigger apparatus (left lower).

The velocity measurement gate is located at the front of tube which models the shaft bottom. Two photoelectric detectors are used for the impact velocity measurement. Figure 4 shows the velocity measurement gate and the photoelectric detectors. A reinforced acrylic tube was used as shaft bottom model in pre-tests. Figure 5 show the ordinary test arrangement of the shaft bottom. The steel tube with 10 mm thick acrylic window describes the shaft bottom. The depth of the shaft bottom model is 1.2 m and the diameter is 400 mm. The real depth of shaft bottom is 20 m and the diameter is 6.5 m.

Fig.4 Velocity measurement gate and photoelectric detector.

Fig. 5 Model of canister shaft bottom.

3.2 Preliminary tests and preliminary test results

In pre-tests 5 experiments were performed with the scale model 1:16 and three experiments with the model in scale 1:11. Figure 6 show the measured velocities as a function of distance. The impact velocities varied from 12 to 25 m/s. The impact velocity is measured by the photoelectric detector and the deceleration is measured with help of high speed video camera through transparent graduated cylinder. Figure 7 shows that the damping is almost negligible because the object moves constant distances in three windows.

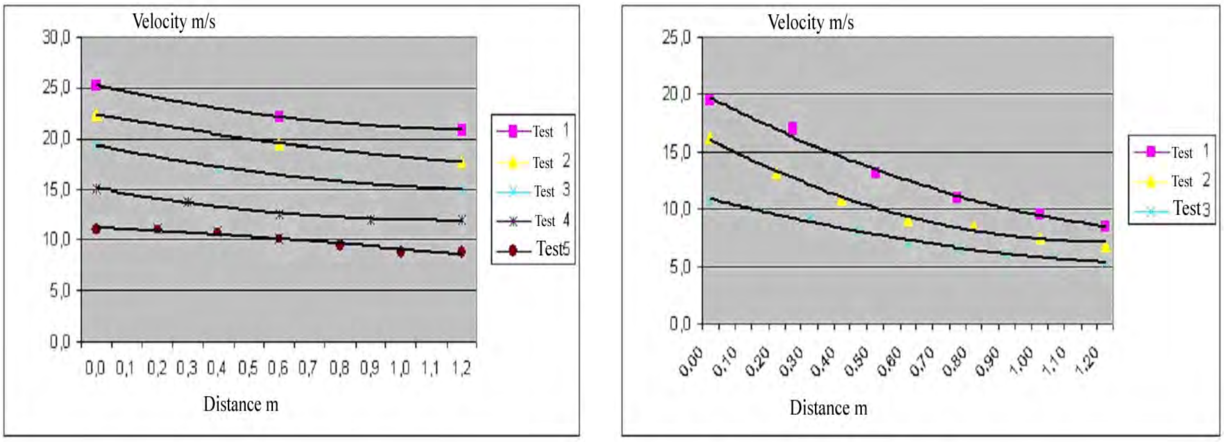

Fig. 6 Velocities as a function of displacement in preliminary test with scale 1:16 (left) and with scale 1:11 (right).

Pre-tests showed that the test piece crashes to the shaft bottom with almost full impact speed and that the terminal velocity is far beyond desired.

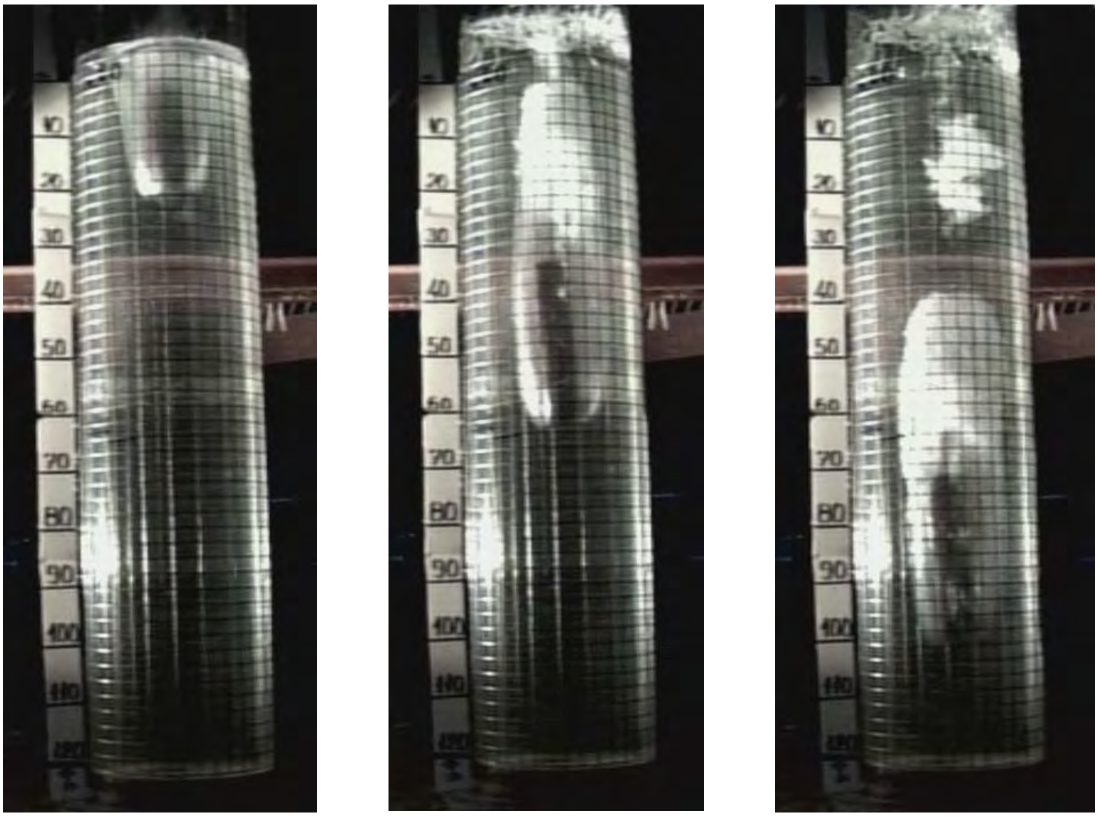

Fig. 7 Test piece entry into water.

4. REAL TESTS AND TEST RESULTS

4.1 Test arrangements

The scale in the real test was 1:16.7. The object diameter is 63 mm and the length 287 mm, Figure 9. The acceleration sensor was fixed in the object. The sensor is capable to measure 500 g's acceleration with 25 kHz sampling frequency.

Fig. 8 Test piece with acceleration sensor. Conical noses used in tests are shown in foreground.

4.2 Real tests

The water does not damp enough the object's movement. Acceptable results were not received. The object withstands without problems the impact on water but the velocity is not decreasing enough even if very high water column is in the shaft bottom. Figure 9 show the measured object movements the respective measured decelerations in water in real scale. The impact velocities were 100 and 82 m/s. Correlation between measured and calculated values is pretty good. The maximum decelerations 60 to 100 m/s^2 encounter at the moment of impact. According these test results it was necessary to start development of the mechanical shock absorber at the bottom of the shaft.

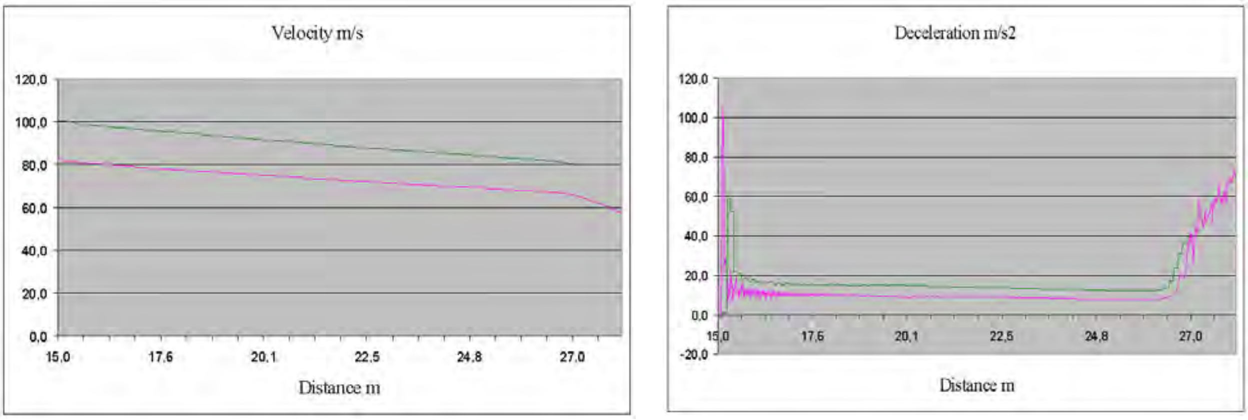

Fig. 9 Measured velocities and decelerations in water in real scale.

4.3 Bottom shock absorber tests

Light Expanded Clay Aggregate (LECA) was selected as shock absorbent material. Six test series, total 29 tests, were performed for development of the shaft bottom shock absorber. In the tests the thickness of the LECA layer was 20 m except in one test series 10 m thick floating LECA layer was used. The thicknesses of the water layer were 0, 10 or 15 m. The shock absorbing capability was also tested with the object's nose cone of 90 or 60 degrees. In these tests wet LECA were used, thickness of water layer was 10 m. The impact velocities were varied from 43 to 126 m/s. Table 1 shows the test parameters of the shaft bottom shock absorber tests.

Table 1. Bottom shock absorber tests.

Test no.	LECA layer m	Water layer m	Water below LECA m	Velocity m/s	Nose chape
1	20	0	0	62	Flat
2	20	0	0	78	Flat
3	20	0	0	100	Flat
4	20	0	0	112	Flat
5	20	0	0	126	Flat
6	20	15	3	43	Flat
7	20	15	3	64	Flat
8	20	15	3	83	Flat
9	20	15	3	102	Flat
10	20	15	3	106	Flat
11	20	15	3	120	Flat
12	10	15	10	43	Flat
13	10	15	10	63	Flat
14	10	15	10	83	Flat
15	10	15	10	105	Flat
16	10	15	10	118	Flat
17	20	10	0	43	Flat
18	20	10	0	64	Flat
19	20	10	0	79	Flat
20	20	10	0	108	Flat
21	20	10	0	123	Flat
22	20	10	0	88	Cone 90^o
23	20	10	0	104	Cone 90^o
24	20	10	0	118	Cone 90^o
25	20	10	0	44	Cone 60^o
26	20	10	0	66	Cone 60^o
27	20	10	0	90	Cone 60^o
28	20	10	0	107	Cone 60^o
29	20	10	0	119	Cone 60^o

The grain size of LECA varied from 4 to 8 mm, Figure 10 (left). The volume density of LECA is about half of the water's density. LECA is not water absorbent material. Wetting is tested with help of tube filled with floating LECA layer 12 (right).

 

Fig.10 LECA as a mechanical shock absorber at the shaft bottom. On right water absorbent test of LECA. The water level is halfway of LECA layer at the point of tape.

4.4 Results of shaft bottom shock absorber tests

LECA was ideal shock absorbing material in all test cases where LECA was not floating. Damping is optimal when the velocity decrease is linear and the deceleration is constant.

4.4.1 Thickness of LECA layer 20 m, dry shaft

Figure 11 and 12 show the velocity and deceleration curves with different impact velocities. Damping is optimal in all impact velocities.

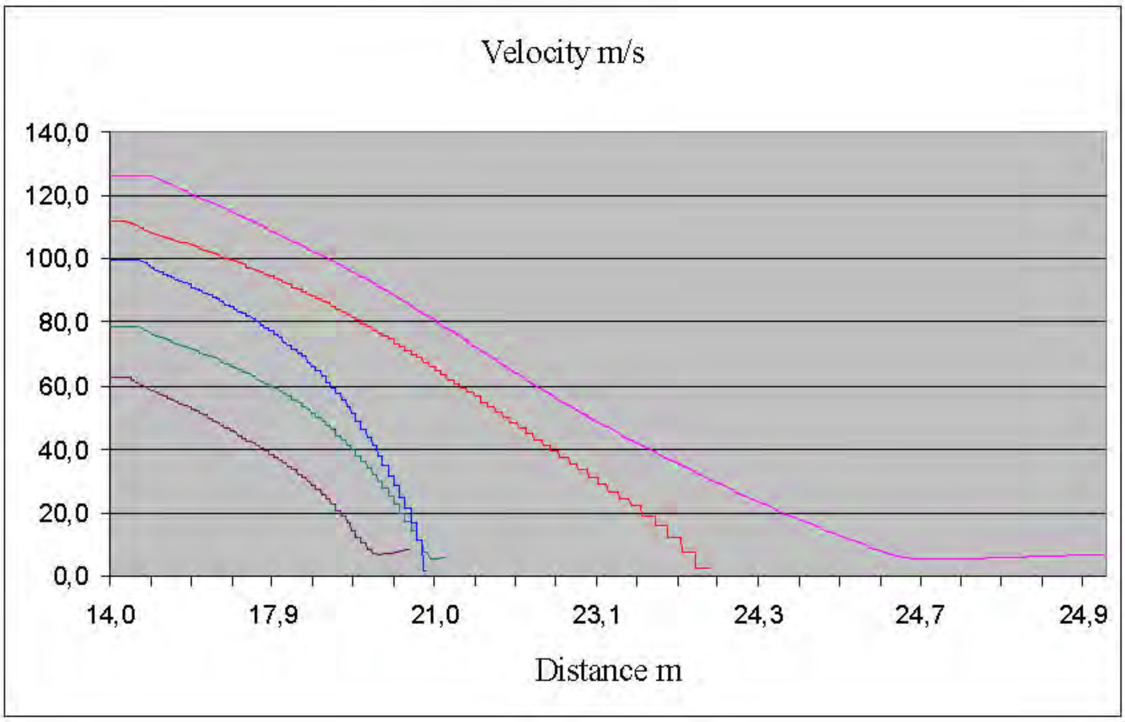

Fig.11 Thickness of LECA layer 20 m, shaft dry, and velocity as a function of distance.

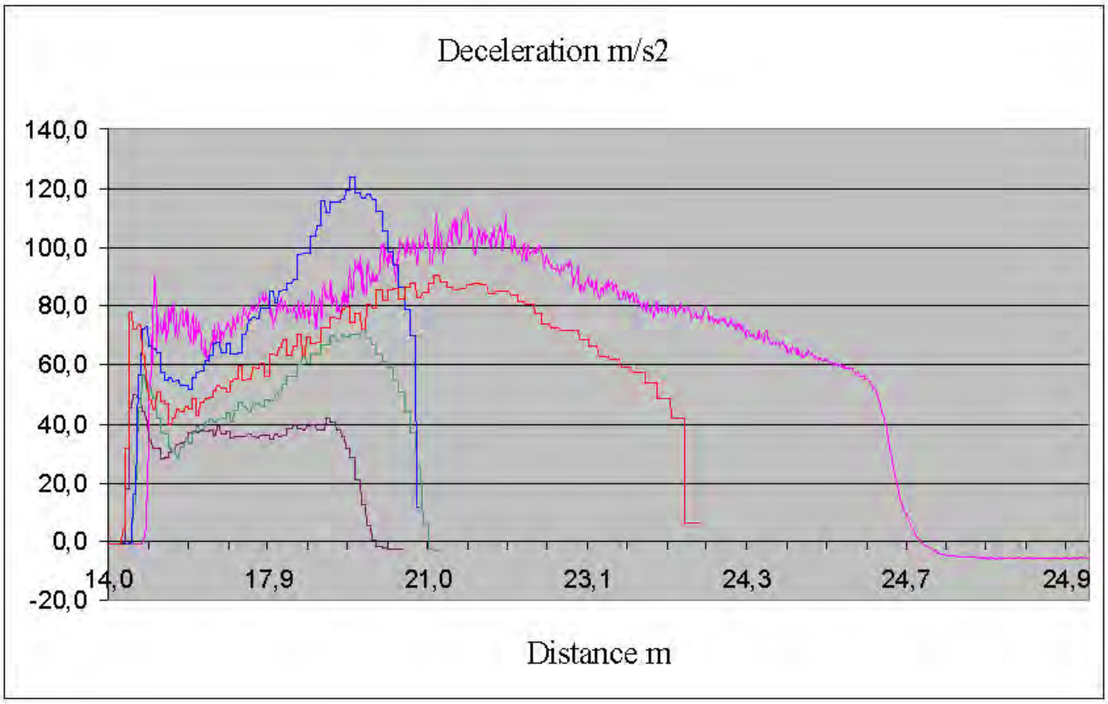

Fig.12 Thickness of LECA layer 20 m, dry shaft, and deceleration as a function of distance.

4.4.2 Thickness of LECA layer 20 m, 3 meters water column

Figure 13 and 14 show the velocity and deceleration curves with different impact velocities. Damping is optimal in all impact velocities.

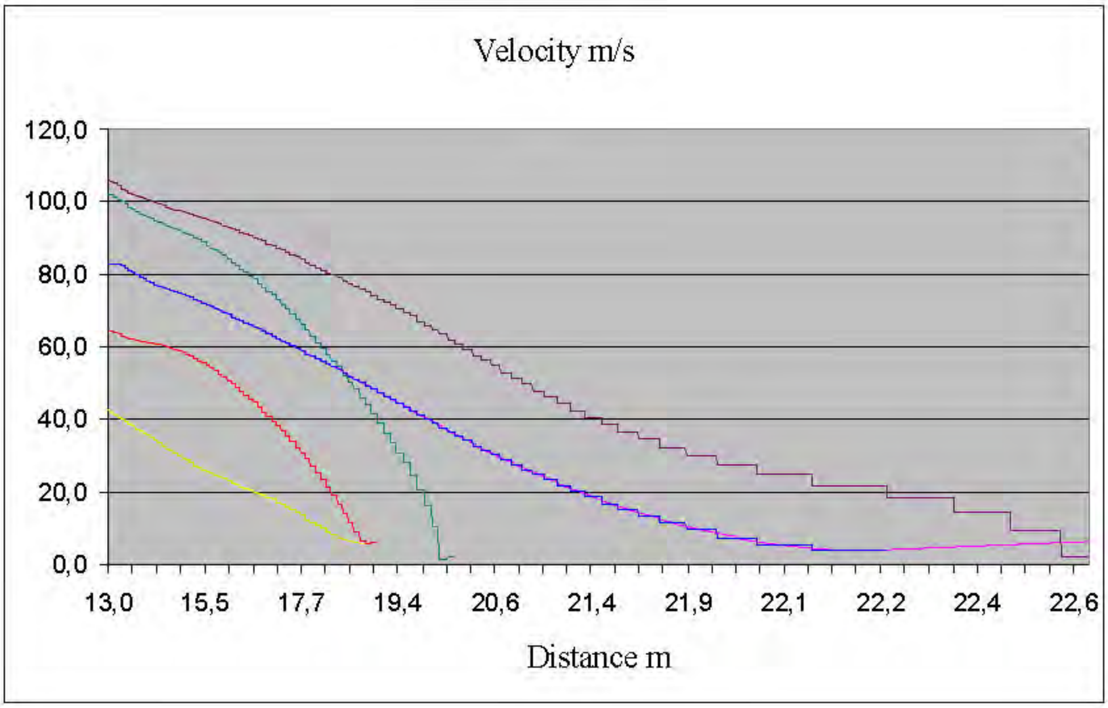

Fig.13 Thickness of LECA layer 20 m, 3 meters water column in shaft, and velocity as a function of distance.

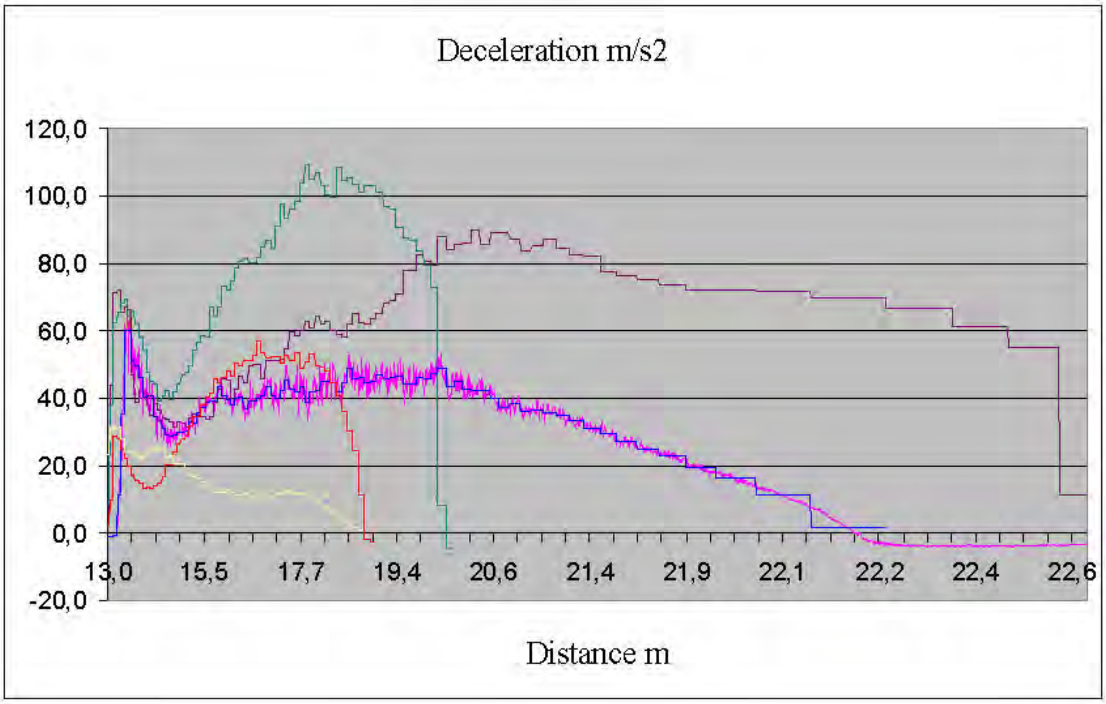

Fig.14 Thickness of LECA layer 20 m, 3 meters water column in shaft, and deceleration as a function of distance.

4.4.3 Thickness of LECA layer 10 m, 10 meters water column

Figure 15 shows the velocity and deceleration curves with different impact velocities. Acceptable test results were not obtained in the test series, where LECA layer was floating. With the maximum and minimum impact velocities the test piece penetrates the LECA layer without stopping and the test piece crashes at the shaft bottom. With other impact velocities the test piece stopped for a moment and then penetrates slowly the LECA layer. LECA layer acts as optimal shock absorber if the LECA layer is thick enough and it is properly supported by the shaft bottom and walls.

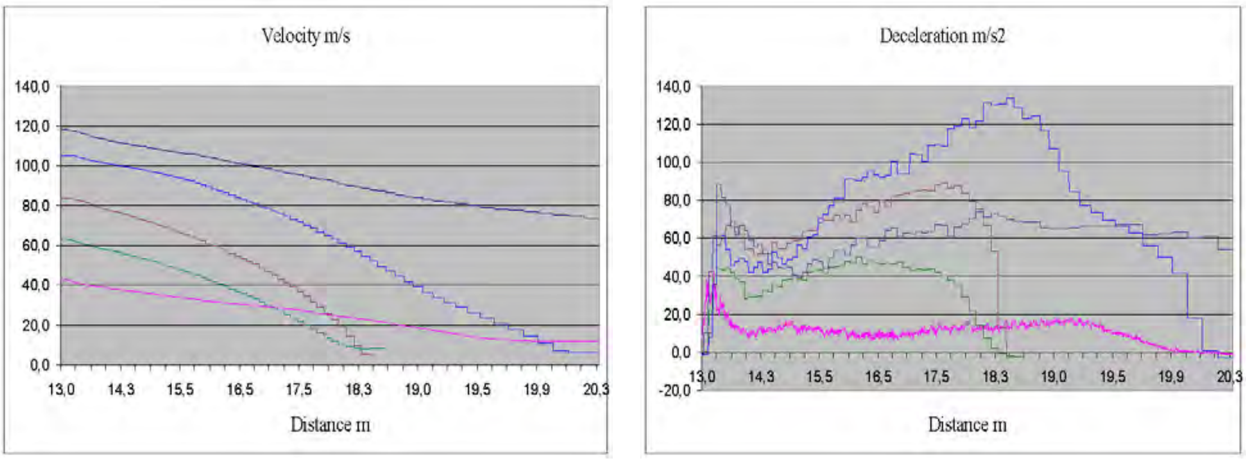

Fig. 1 Thickness of LECA layer 10 m, 10 meters water column in shaft, velocity and deceleration as a function of distance.

4.4.4 Wet LECA layer 20 m

Figure 16 show the velocity and deceleration curves with different impact velocities. Damping is optimal in all impact velocities.

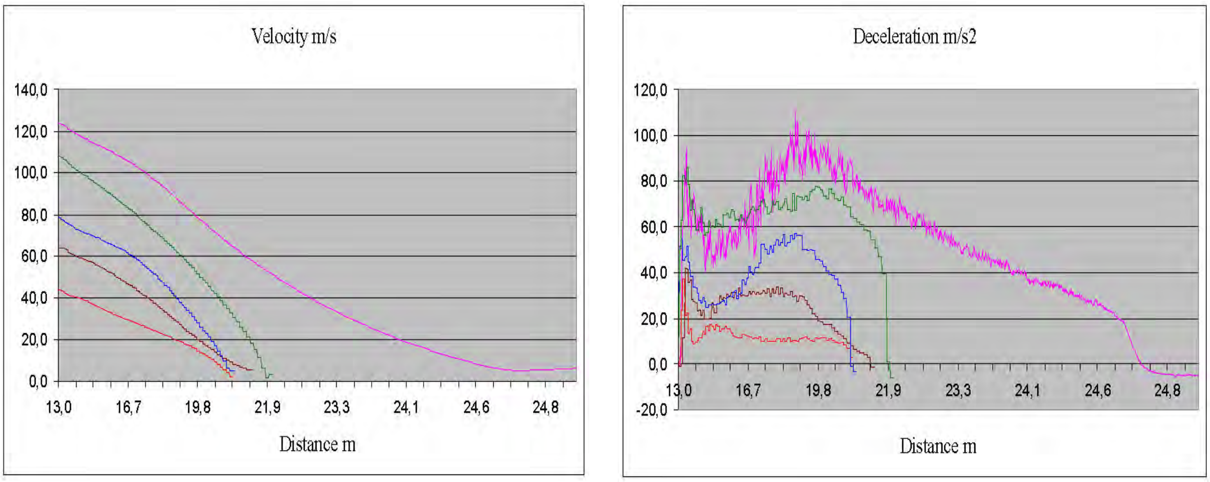

Fig. 2 Wet LECA layer 20 m, velocity and deceleration as function of distance.

4.4.5 Wet LECA layer 20 m, nose cone of 90 degree

Figure 17 show the velocity and deceleration curves with different impact velocities. Damping is optimal but the nose cone does not give any advantages.

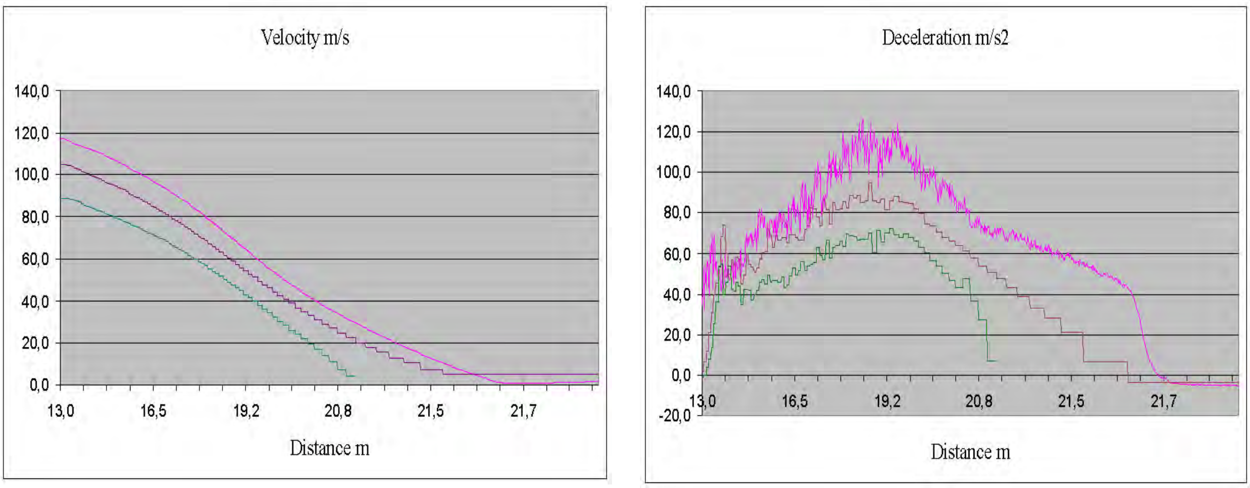

Fig. 3 Wet LECA layer 20 m, 90^{o} nose cone, velocity and deceleration as function of distance.

4.4.6 Wet LECA layer 20 m, nose cone of 60 degree

Figure 18 show the velocity and deceleration curves with different impact velocities.

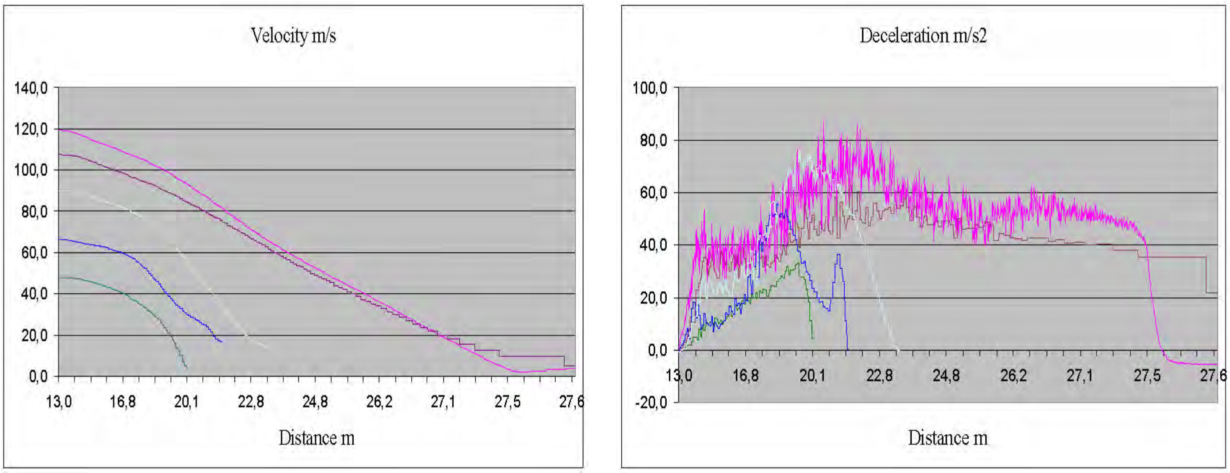

Fig. 4 Wet LECA layer 20 m, 60^o nose cone, velocity and deceleration as function of distance.

The nose cone decreases the decelerations on the expenses of braking distance. It is not necessary to reshape the canister bottom; the original flat shape is good enough.

5 CONCLUSIONS

Canister lift can be intentionally damaged and the fuel canister is falling into the canister shaft. The maximum falling height is about 500 m. The fuel canister may reach 100 m/s impact velocity.

The water layer at the bottom of the canister shaft will not decrease the canister velocity enough even with tens of meters' water layer. Mechanical shock absorber at the bottom of the shaft is needed.

At the bottom of the shaft 20 m thick LECA layer acts as optimal shock absorber. Canister remains intact with all impact velocities. It is not necessary to reshape the fuel canister bottom. There is also no need for canister nose cone.

The leakage water level at the canister shaft bottom shall be limited to the level where the LECA layer is not floating because the canister can penetrate the floating LECA layer with high and low impact velocities. When the water level is limited into two thirds of LECA layer's height then the LECA layer is not floating and damping is optimal.

REFERENCES

[1] Bruce R. Munson, Donald F. Young and Theodore H. Okiishi. ”Fundamentals of fluid mechanics”. John Wiley & Sons, New York, Chichester, Brisbane, Toronto, Singapore. 1990.
[2] Kukkola, T. and Törmälä, V-P. "Shaft shock absorber tests for a spent fuel canister. Working Report 2003-53. Posiva Oy, Olkiluoto, October 2003. (in Finnish)
[3] Sedov, L. I. ”Similarity and dimensional methods in mechanics”. MIR Publishers Moscow. 1982.
[4] Kornhauser, M. ”Structural effects of impact”. Spartan Books, Inc. Baltimore and Cleaver-Hume Press London. 1962.